

Fast-moving electrostatic solitons in a plasma with turbulence heating

Mridusmita Das¹, Murchana Khusroo², Madhurjya P. Bora^{1*}

^{1*}Department of Physics, Gauhati University, Guwahati, 781014, India.

²Department of Physics, University of Science & Technology Meghalaya,
Ri-Bhoi, 793101, India.

*Corresponding author(s). E-mail(s): mpbora@gauhati.ac.in;

Abstract

In this work, it is shown that electrostatic solitons in a plasma with turbulent heating of the electrons through an accelerating electric field can form with very high velocities, reaching up to several order of magnitudes larger than the equilibrium ion-sound speed. The possible parameter regime, where this work may be relevant, can be found in the so-called “dead zones” of a protoplanetary disk. Though these zones are stable to magnetorotational instability, the resultant turbulence can in fact heat the electrons making them follow a highly non-Maxwellian velocity distribution. We show that these fast-moving solitons can reach very high velocities. With electron velocity distribution described by the Davydov distribution function, we argue that these solitons can be an effective mechanism for energy equilibration in such a situation through soliton decay and radiation.

Keywords: soliton, turbulence

1 Introduction

In this work, we consider the plasma environment of a protoplanetary disk and the formation of electrostatic solitons in such a plasma. In these plasmas, there can be turbulence-driven electric field causing random heating of the electrons pushing the electrons to have a highly non-Maxwellian distribution. Protoplanetary disks (PPD) are circumstellar disks around young stars, which usually precede the formation of planets. These disks are primarily made up of gas, dust, and debris, which eventually

break up to give rise to planets and similar smaller orbiting objects around the parent star [1–4]. They are formed around the equatorial plane of the star with radii ranging to several AUs. They are also quite cold objects with temperatures gradually falling from about 1000 K to about 100 K as one goes out from the inner to the outer regions of the disk [5, 6]. Apart from being weakly ionized plasmas, the environment of a PPD also contains a considerable amount of dust grains. The electrostatic interaction between the dust grains and the plasma can give rise to various plasma processes which can considerably affect the resulting nonlinear interactions [7]. In recent years, we are observing a renewed interest in studying PPDs, primarily due to their important roles in the formation of planets and recent advances in space technology which have led to the discovery of several exoplanets. However, the exact mechanisms which eventually break down a PPD leading to planet formation, can still be debated about, as there are several competing processes which can simultaneously develop to form a quite complex scenario. Although the magnetorotational instability (MRI) [8, 9] is believed to be a major candidate for the reorganization of disk material, the presence of dust grains creates the so-called “dead zones” where MRI can no longer operate. In contrast to the dead-zones, there is an “active zone”, which is a turbulent envelope of plasma that surrounds the dead zone [10]. We should also note that the ambient large-scale magnetic field in a PPD is actually very small, about a Gauss at ~ 1 AU to a few milli-Gauss, as one moves out to the extreme outer region [11]. In the outer region, the magnetic field is so weak that no observational evidence of the magnetic field could be detected through related phenomena such as the Zeeman effect [5].

The coupling between a moving plasma and magnetic field through MRI-driven turbulence can produce a finite electric field, even in a dead zone, which can be quite strong. In a weakly ionized plasma such as in the outer region of a PPD, such an electric field, if sufficiently strong, can produce random motion and cause heating [12]. The acceleration of the electrons by this electric field is balanced due to the collisional loss of energy and momentum with the neutrals. Though these collisions can both be elastic and inelastic, the loss of energy due to inelastic collisions can be largely ignored for energies $\lesssim 1$ eV [13]. This approximation allows the electron velocity distribution to be written in a form which is known as *Davydov* distribution [13–16]. On the other hand, the ion distribution function still remains largely Maxwellian [13]. If we can ensure electrical quasi-neutrality (see the discussion on the validity of quasi-neutrality in Section 3.1) in such a plasma with the relevant timescale (ion-acoustic), we can describe it with the ion fluid equations, stationary dust grains, and electrons with Davydov distribution function. The charged dust grains affect the plasma dynamics by depleting the electrons and by maintaining a static electrical background.

Coming to the subject of nonlinear electrostatic structures like solitons, envelope solitons, and shock waves, we note that they are of very special interest to plasmas. Usually, in both space and laboratory plasmas, the turbulence becomes high enough such that nonlinear and dispersion effects become comparable and localized electrostatic structures like solitons and envelope solitons start to form [17]. However, it is now well known that plasma solitons are almost always unstable [18] and can be an effective mechanism for energy equilibration through processes like soliton radiation, where a soliton effectively *radiates* ion-acoustic waves, which in turn causes

the soliton amplitude and velocity to decrease [19, 20]. In this work, we show that in a situation, where turbulence-driven heating can change the effective electron distribution function, large-amplitude electrostatic solitons can form and can reach very high velocities up to several orders of magnitude higher than the equilibrium ion-sound velocity. These large, fast-moving solitons can then be very effective pathways for energy transfer in such a plasma. As discussed above, these solitons can form in the “dead zones” and transfer energy outward. In Section 2, we briefly discuss the theory of MRI turbulence and plasma heating [13]. We also discuss the relevant parameter regime where our analysis can be useful, toward the end of this section. In Section 3 and the subsequent subsection, we formulate the electron velocity distribution and the electron density. We discuss the nonlinear electrostatic waves in Section 4 and also discuss the possible effects of dust-charging. In Section 5, we briefly discuss the behaviour of nonlinear electrostatic waves when no dust is present. In Section 6, we discuss the full implications of dust effects and discuss the most important findings of this analysis. In this section, we also outline a mathematical procedure, which can be used to make the analytical interpretation of these waves easier. In Section 7, we conclude.

2 Debye-scale structures in a turbulent plasma

Turbulence is one of the most common and universal nonlinear phenomena observed in naturally occurring fluids. In electrically active fluid like plasma, electrostatic and electromagnetic turbulence are routinely observed in space plasmas such as solar wind, plasmas in the magnetosphere, interplanetary plasmas, as well as in laboratory plasmas [21]. While different manifestations of nonlinear phenomena like shock waves (both dissipation and dissipation-less), solitons, and double layers can occur independent of each other, a turbulent regime can give rise to all these under suitable environment. In general, a turbulent flow is characterised by the so-called inertial subrange where large-scale eddies feed energy into successively smaller eddies, before the energy is dissipated away through viscous drag. Naturally, viscosity does not play any significant role during the inertial subrange. This inertial subrange can be compared to what is known as local thermodynamic equilibrium (LTE) in the context of energy flow in stellar interiors where an ‘equilibrium’ is achieved despite continuous energy flow from the centre of a star to its outer areas maintained at a constant gradient of temperature [22, 23].

In fact, appearances of coherent structures in turbulent flow have been intriguing scientists for a long time. A very detailed overview of solitons in a turbulent flow can be found in the review article by Levich [24, 25]. It is now believed that accumulation of energy at large scales is intuitively favourable to the birth of coherent structures in a turbulent environment. There are also plenty of observational evidences where soliton-like coherent structures (SCS) are observed in low-speed turbulent boundary layers [26–29], which are believed to be results of streak instability and hairpin vortex. Other examples of coherent structure such as solitons in a turbulent flow include vortex solitary waves in a rotating turbulent flow [30]. As far as space plasmas are concerned, SCS are routinely observed in the form of ion and electron holes. A very

recent observation of such example through Parker Solar Probe (PSP) is reported by Mozer et al. [31] in near-sun solar wind plasmas, though such observations in ion-acoustic regime have also been reported earlier [32]. Coherent structures are also reported to be seen in fusion plasmas [33–36], where imaging of the edge region of tokamaks shows localized filaments [33, 34]. In a charged fluid like plasma, bipolar electric fields are routinely observed within a turbulent regime in magnetospheric and solar wind plasmas indicating development of Debye-scale potential structures. Recent observations of Magnetospheric Multiscale (MMS) spacecraft of bipolar electrostatic structures indicates that these structures are formed through turbulence, driven by Buneman instability which provides energy to the accelerating ions in Earth’s bow shock regions [37, 38]. These bipolar electric fields are results of an electrostatic potential hump or electrostatic solitons arising out of this turbulent equilibrium. Very recent numerical simulation also indicates that external charged debris can cause localised solitons known as pinned solitons formed out of ion-ion counter-streaming turbulence [39]. In any case, we can very well consider the formation of electrostatic potential hump in an otherwise turbulent flow. Mathematically, this is equivalent to considering an electrostatic perturbation in an equilibrium background. We argue that this must happen within the energy spectrum of the inertial subrange of the turbulence as viscosity does not seem to play a significant role in formation of these structures.

We now recall that an electrostatic potential hump or electrostatic soliton can be mathematically described by a pseudo-potential $V(\phi)$ through the well-known Sagdeev potential equation

$$\frac{d^2\phi}{dx^2} = f(\phi) = -\frac{dV}{d\phi}, \quad (1)$$

which is basically a re-framed version of Poisson’s equation for electrostatic potential ϕ . In the weak nonlinearity limit, this equation can be reduced to a Korteweg-de Vries (KdV) equation [40] which admits the well-known ‘sech’ solution depicting a soliton. We should note here that while the KdV equation is fully integrable, another widely used, non-integrable equation which also admit a ‘sech’ solitary wave solution is the regularized-long-wave (RLW) equation, first proposed by Peregrine in 1966 [41]. In fact, in the small wave number limit the RLW equation reduces to a KdV equation. We, in this work, however describe our solitary structure through the pseudo-potential equation.

3 MRI turbulence and plasma heating

In this section, we briefly review the physics of local heating of the electrons in a weakly ionized plasma due to the strong electric field generated through MRI turbulence in an environment similar to a PPD, as discussed in details by Okuzumi and Inutsuka [13].

We consider an $e-i$ plasma with a considerable presence of neutrals. As with any plasma, we expect the plasma particles to thermalize with the neutrals when there is no external force field present in the plasma. The situation becomes vastly different in the presence of an external electric field. Though both electrons and ions get accelerated in the opposite directions by the field, effective electrons are heavily accelerated due to their high mobility. Besides the energy transfer during binary collisions between the

electrons and neutrals is quite low [13]. It can be proved that in this scenario [15, 42], one can attain an equilibrium if the magnitude of the electric field E exceeds a certain critical value

$$E_{\text{crit}} = \left(\frac{T_n}{el_e} \right) \sqrt{\frac{6m_e}{m_n}}, \quad (2)$$

where $l_e = (n_n \sigma_{en})^{-1}$ is the electron mean free path and σ_{en} is the electron-neutral momentum-transfer cross section [43] and the ‘ n ’ subscript denotes the neutrals. In this case the random thermal energy of the electrons heavily overwhelms that of the neutrals $v_{\text{the}} \gg \sqrt{T_n/m_n}$. For a hydrogen-rich environment with $\sigma_{en} \sim 10^{-15} \text{ cm}^2$ at electron energy $< 10 \text{ eV}$, we have [44, 45]

$$E_{\text{crit}} \sim 10^{-9} T_{100} n_{12} \text{ esu cm}^{-2}. \quad (3)$$

In the above relation, T_{100} is the temperature measured in terms of 100 K and n_{12} is the neutral number density measured in terms of 10^{12} cm^{-3} . It can be shown that [13]

$$\frac{E_{\text{MRI}}}{E_{\text{crit}}} \approx \frac{200}{\Lambda} \left(\frac{100}{\beta_z} \right) n_{12}^{-1/2}, \quad (4)$$

where E_{MRI} is the strength of the electric field, generated due to MRI turbulence in a situation like that of a PPD. It should be noted that the above expression is independent of the gas temperature T , where

$$\Lambda = \frac{v_{Az}^2}{\eta \Omega} \quad (5)$$

is the Elsasser number [46] – the ratio of the kinetic energy to the Coriolis energy, β_z is the plasma β of the vertical magnetic field, and v_{Az} is the corresponding Alfvén velocity. An upper limit for Λ can be established by noting the fact that for electron heating, one must have $E_{\text{MRI}} > E_{\text{crit}}$. However, for sustaining the MRI-driven turbulence, E_{MRI} has to be sufficiently strong, from which we have the condition that $\Lambda > \Lambda_{\text{crit}}$. Naturally, for a sustained MRI-driven turbulence heating of the electrons, we must have [13],

$$\Lambda_{\text{crit}} \lesssim \Lambda \lesssim 200 \left(\frac{100}{\beta_z} \right) n_{12}^{-1/2}. \quad (6)$$

We note in a typical situation of a PPD, $\Lambda \sim 0.1 - 1$ and $n_{12} \sim 10^2 - 10^6$ with $\beta_z \sim 100 - 1000$, and the above condition can be readily satisfied.

3.1 Plasma parameters and validity

It is necessary to validate the parameter space and validate the assumptions that we make in subsequent sections. PPDs are weakly ionized structures with considerable presence of neutrals and dust grains. There is also a considerable amount of ion-neutral and electron-neutral collisions. Considering the characteristic scale length and timescale, we can now estimate the basic plasma parameters for this plasma, which are Debye length (λ_D), plasma frequencies ($\omega_{p,j}$) and mean collision times (τ_j) for

different species, $j = i, e, d$ for ions, electrons, and dust particles. The Debye length can be parameterized as [5]

$$\lambda_D = \frac{3}{10} \xi_{-13}^{-1/2} R_{\text{AU}}^{7/8} (1 + Z)^{-1/2} \text{ m}, \quad (7)$$

where ξ_{-13} is the ionization fraction n_-/n_n , the ratio of free negative charge carriers n_- and neutrals n_n , measured in the units of 10^{-13} , R_{AU} is the radial distance from the center of the PPD in the units of AU, and Z is the ion charge number. The quantity ξ_{-13} is a highly uncertain quantity, which can be estimated to $\sim 1 - 10^{-3}$. With $Z = 1$ and $R_{\text{AU}} \sim 1$, we have $\lambda_D \sim 1 - 30 \text{ m}$ [5, 47], which is clearly quite smaller than the relevant scale lengths in question. Apparently, the number of particles in the Debye sphere $\sim 10^6 \gg 1$. So, these objects can still be considered very much in the plasma regime even though they have a very low ionization and temperature [5]. This approximation can of course break down at higher charge number $Z \gtrsim 10^3$, which is however prohibitively large [11].

Coming to the question of quasi-neutrality, which is of course assumed throughout this work, it is important to justify its validity region. We consider the electron and ion plasma frequencies, which can be parameterized as [5]

$$\omega_{p,e} = 2.2 \times 10^5 \xi_{-13}^{1/2} R_{\text{AU}}^{-9/8} \text{ s}^{-1}, \quad (8)$$

$$\omega_{p,i} = 9.3 \times 10^2 \xi_{-13}^{1/2} R_{\text{AU}}^{-9/8} \text{ s}^{-1}, \quad (9)$$

and the corresponding average mean collision times

$$\tau_{s,e} = 6.7 \times 10^{-7} R_{\text{AU}}^{9/4} \text{ s}, \quad (10)$$

$$\tau_{s,i} = 4.9 \times 10^{-5} R_{\text{AU}}^{9/4} \text{ s}. \quad (11)$$

With the relevant parameters for PPD, one can show that $10^{-2} < \omega_p \tau_s < 1$, and it can be concluded that electrical quasi-neutrality is recovered on timescales shorter than a second [5]. So, we can safely conclude that quasi-neutrality is maintained by electrons and neutrals, at least, in the ion-acoustic timescale.

The probable region of the PPD, where this work might be of relevance is toward the outer edge of the disk where the plasma is only weakly ionized and there exists a so-called MRI-stable “dead zone” [5, 13]. However, it has been shown that the MRI-driven turbulence can produce an electric field in the neutral co-moving frame when ionization is low. In these regions the large-scale magnetic field is quite weak $\sim 10 \text{ mG}$ [5]

$$B \sim 12 R_{\text{AU}}^{-11/8} \beta^{-1/2} \text{ G}, \quad (12)$$

so that the thermal pressure dominates over magnetic pressure, resulting a very high plasma $\beta \gg 1$, which the ratio of the thermal pressure to that of the magnetic field. From which, we see that the electron and ion gyro-radii $\gg \lambda_d$ and a localized electrostatic structure can form.

4 Electron distribution and heating

Let us now consider the Davydov velocity distribution function for the electrons. This distribution function can be considered as an equilibrium distribution function in a turbulent environment with the assumption that fluctuations within the distribution function itself can be considered to be a part of the equilibrium distribution function provided the relaxation timescale for these fluctuations is considerably less than kinetic timescale on which the distribution function itself may evolve [13, 15, 16, 43].

This distribution function can be written as [16]

$$f_e(\mathbf{E}, \mathbf{v}) = \left(1 - \frac{eEl}{T} \frac{\epsilon \hat{\mathbf{E}} \cdot \hat{\mathbf{v}}}{\epsilon + \chi T}\right) f_{e0}(E, v), \quad (13)$$

where $\epsilon = 1/2(m_e v^2)$ is the kinetic energy of the electrons having velocity \mathbf{v} and χ is a dimensionless quantity defined as the square-root of the ratio of the electric field E to its critical value

$$\chi = \left(\frac{E}{E_{\text{crit}}}\right)^2. \quad (14)$$

In Eq.(13), $\hat{\mathbf{E}} = \mathbf{E}/E$, $\hat{\mathbf{v}} = \mathbf{v}/v$, and

$$f_{e0} = \left(\frac{m_e}{2\pi T}\right)^{3/2} \frac{(\epsilon/T + \chi)^\chi}{\mathcal{W}(\chi)} e^{-\epsilon/T}, \quad (15)$$

where

$$\mathcal{W}(\chi) = \chi^{3/2+\chi} U\left(\frac{3}{2}, \frac{5}{2} + \chi, \chi\right). \quad (16)$$

The functions $U(x, y, z)$ is the confluent hypergeometric function of the second kind [13]. As we note, $f_{e0}(E, v)$ is the symmetric part of $f_e(\mathbf{E}, \mathbf{v})$ that depends on the magnitudes of \mathbf{E} and \mathbf{v} but not on the angle between them $\cos^{-1}(\hat{\mathbf{E}} \cdot \hat{\mathbf{v}})$. In the limit of weak electric field ($E \ll E_{\text{crit}}$), f_{e0} reduces to the usual Maxwellian distribution,

$$f_{e0}^M = \left(\frac{m_e}{2\pi T}\right)^{3/2} e^{-\epsilon/T}. \quad (17)$$

In the limit of a strong electric field ($E \gg E_{\text{crit}}$), f_{e0} reduces to the Druyvesteyn distribution function [42],

$$f_{e0}^D = \frac{1}{\pi\Gamma(3/4)} \left[\frac{3m_e^3}{4m_n(eEl_e)^2}\right]^{3/4} \exp\left[-\frac{3m_e\epsilon^2}{m_n(eEl)^2}\right]. \quad (18)$$

We now introduce a turbulence-generated electrostatic potential ϕ , expressed in terms of the equivalent electrostatic energy $\epsilon_p = e\phi$. The distribution function in Eq.(13) becomes,

$$f_e(\mathbf{E}, \mathbf{v}) = \left[1 - \frac{eEl_e}{T} \frac{(\epsilon - \epsilon_p) \hat{\mathbf{E}} \cdot \hat{\mathbf{v}}}{\epsilon - \epsilon_p + \chi T}\right] f_{e0}, \quad (19)$$

where, the symmetric and the asymmetric parts of the distribution function can be written as [43],

$$f_{e0} = \left(\frac{m_e}{2\pi T} \right)^{3/2} \frac{[(\epsilon - \epsilon_p)/T + \chi]^\chi}{\mathcal{W}(\chi)} e^{-(\epsilon - \epsilon_p)/T}, \quad (20)$$

$$f_{\text{asym}}(\mathbf{E}, \mathbf{v}) = -\frac{eEl_e}{T} \frac{(\epsilon - \epsilon_p)}{\epsilon - \epsilon_p + \chi T} \hat{\mathbf{E}} \cdot \hat{\mathbf{v}} f_{e0} \quad (21)$$

The corresponding electron density can be calculated by taking the zeroth order moment of the distribution function,

$$n_e = \int_{-\infty}^{+\infty} f_e(\mathbf{E}, \mathbf{v}) d^3v \quad (22)$$

The above integral in spherical coordinate can be written as [48],

$$n_e = \int_0^{2\pi} \int_0^\pi \int_0^\infty v^2 \sin \theta f_e(\mathbf{E}, v) d\varphi d\theta dv \quad (23)$$

where, the volume element of each spherical shell is $4\pi v^2 dv$. However, noting that $\hat{\mathbf{E}} \cdot \hat{\mathbf{v}} = \cos \theta$, we can see that the integration of the asymmetric part of the distribution function evaluates to zero, so that the electron density is entirely due to the symmetric part of the distribution function

$$\begin{aligned} n_e &= \int_0^\infty 4\pi v^2 f_{e0} dv, \\ &= e^{\epsilon_p} \frac{U\left(-\chi, -\frac{1}{2} - \chi, -\epsilon_p + \chi\right)}{U\left(-\chi, -\frac{1}{2} - \chi, \chi\right)}, \quad \chi > \epsilon_p \end{aligned} \quad (24)$$

where we have re-scaled the energies $(\epsilon, \epsilon_p) \rightarrow (\epsilon, \epsilon_p)/T$. The effect of plasma heating remains in the form of change of magnitude of electron momenta. Also note that the electron density is normalized by its equilibrium value, so that $n_e \rightarrow 1$ when $\epsilon_p \equiv \phi \rightarrow 0$.

4.1 Linear dispersion

In this subsection, we very briefly review the effect of Davydov electrons [14–16] on the linear ion-acoustic dispersion relation. The relevant equations in this case are ion continuity and momentum equations and Poisson equation [48], which can be written

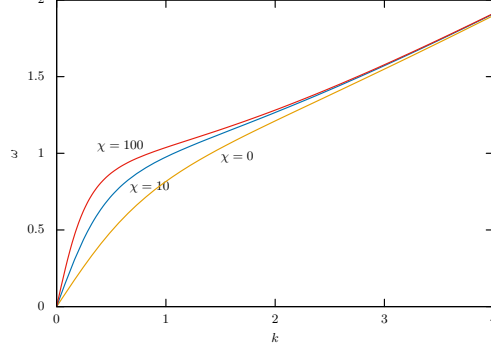


Fig. 1 The linear ion-acoustic dispersion curves for Davydov electrons. All the curves are with $\gamma = 5/3$ and $\sigma = 0.1$.

in the dimensionless form as

$$\frac{\partial n_i}{\partial t} + \nabla \cdot (n_i \mathbf{u}_i) = 0, \quad (25)$$

$$n_i \frac{d\mathbf{u}_i}{dt} = -\nabla \phi - \nabla p_i, \quad (26)$$

$$\nabla^2 \phi = n_i - n_e, \quad (27)$$

where $p_i \propto n_i^\gamma$ is the ion equation of state with γ as the polytropic index and ϕ is the first order turbulence-generated electrostatic potential. The electrons can be considered to be inertial-less and is expressed through Eq.(24). Without loss of any generality, we can use a frame of reference where the equilibrium ion velocity is zero. Expressing a linear perturbation of the form $f \rightarrow f_0 + f_1$ where $f_{0,1}$ are the equilibrium and first-order perturbed quantities with $f_1 \sim e^{-i\omega t + i\mathbf{k} \cdot \mathbf{r}}$. The first order perturbed quantities are represented by $f_1 = (n_{i1}, n_{e1}, u_{i1}, p_{i1}, \phi \equiv \phi_1)$. Following the standard procedure, the linear dispersion relation can be expressed

$$\omega = k \left(\sigma \gamma + \frac{1}{\mathcal{A} + k^2} \right)^{1/2}, \quad (28)$$

where Eq.(24) is linearised as

$$n_{e1} = \mathcal{A} \phi_1, \quad (29)$$

with

$$\mathcal{A} = 1 - \frac{U\left(\frac{3}{2}, \frac{3}{2} + \chi, \chi\right)}{U\left(\frac{3}{2}, \frac{5}{2} + \chi, \chi\right)}. \quad (30)$$

In the above equations, we have normalised the densities by their respective equilibrium values, ϕ_1 by T_e/e , ω by c_s/λ_D , and k by λ_D^{-1} . λ_D is the electron Debye

length and $\sigma = T_i/T_e$. We can easily see that in the limit $\chi \rightarrow 0$, $\mathcal{A} \rightarrow 1$, the electrons become Boltzmannian and we recover the usual ion-acoustic dispersion relation.

In Fig.1, we have shown the linear dispersion curves for Davydov electrons. As can be seen, a higher χ makes the ion-acoustic wave behave like a constant frequency wave for lower σ .

5 Nonlinear electrostatic waves

When considering the formation of nonlinear electrostatic waves in such a plasma, we assume that scale length of electrostatic structures is smaller than the average turbulence scale length due to MRI, so that the effect of turbulence on these structures can be safely neglected. Thus, our plasma model consists of cold ions and non-inertial electrons obeying Davydov velocity distribution. Though the negatively charged dust particles is an integral component of the plasma in our model in the ion-acoustic time scale, dust dynamics can be neglected. However, their presence is quite necessary for the overall charge-balance. The primary equation is the Poisson equation (dimensional),

$$\epsilon_0 \frac{\partial^2 \phi}{\partial x^2} = e(n_e - n_i + z_d n_d), \quad (31)$$

where z_d is the dust-charge number and n_d is the dust density. The dust density remains constant, though the dust-charge number z_d must be determined self-consistently using the electron-ion current balance equations to the dust particles. Following energy conservation for the ions, the ion density n_i can be written as,

$$n_i = n_{i0} \left(1 - \frac{2e\phi}{m_i u_0^2} \right)^{-1/2}, \quad (32)$$

where we have assumed the ions to be cold and u_0 is the ion velocity at ∞ . The electron density is now given by Eq.(24). As before, we choose to normalize the ion density by its equilibrium values $n_i = n_{i0}$, the plasma potential by T_e/e and length by Debye length λ_D . Far away from the perturbation, the plasma potential vanishes, and we define the boundary conditions as $\phi \rightarrow 0$ at $x \rightarrow \infty$ and the normalized Poisson equation becomes,

$$\frac{\partial^2 \phi}{\partial x^2} = n_e - \delta_i n_i + \delta_d z_d = F(\phi), \quad (33)$$

where $\delta_i = n_{i0}/n_{e0}$ and $\delta_d = n_{d0} z_{d0}/n_{e0}$. The dust-charge number z_d is scaled as $z_d \rightarrow z_d/z_{d0}$, where z_{d0} is the equilibrium value of $z_d|_{\phi=0}$. Multiplying the above equation by $d\phi/dx$ and integrating we have,

$$\frac{1}{2} \left(\frac{d\phi}{dx} \right)^2 = \int_0^\phi F(\psi) d\psi = -V(\phi), \quad (34)$$

where $V(\phi)$ in Eq.(34) represents Sagdeev or the pseudo-potential [49]. The limits of the above integration ensure that Sagdeev potential obeys the boundary condition at $\phi = 0$, namely $V(\phi = 0) = 0$.

In the case of pure Maxwellian electrons, $n_e = e^\phi$ and the integrations for electron and ion contributions in the above equation can be carried out analytically and we have an expression for Sagdeev potential as,

$$V(\phi) = 1 - e^\phi + \delta_i M^2 \left(1 - \sqrt{1 - \frac{2\phi}{M^2}} \right) - \delta_d I_d(\phi), \quad (35)$$

where $M = u_0/\sqrt{T_e/m_i}$ is the ion Mach number and

$$I_d(\phi) = \int_0^\phi z_d(\psi) d\psi \quad (36)$$

is the contribution of the dust particles to the pseudo-potential. We note that the integral in Eq.(34) can not be carried out analytically and has to be evaluated numerically.

A clarification on the definition of Mach number *must* be given at this point. The Mach number here is defined in the case of usual ion-acoustic speed for an Maxwellian electron-ion plasma. It has been argued in the literature that the Mach number needs a re-definition in terms of the acoustic speed, defined in terms of the linear ion-acoustic dispersion relation as

$$M = u_0/c_{\text{dis}}, \quad (37)$$

where c_{dis} is the ion-acoustic speed determined from the linear dispersion relation

$$c_{\text{dis}} = \lim_{k \rightarrow 0} \frac{\omega}{k} \equiv \lim_{k \rightarrow 0} \frac{d\omega}{dk}. \quad (38)$$

In this work, however, we shall continue to define the Mach number with its so-called classical definition and will be careful about comparing the soliton velocity *only* with the classical ion-acoustic speed.

5.1 Dust contribution

In order to evaluate the integral given in Eq.(36), we assume that the net current (electron and ion) to the dust particles remains zero

$$\sum_{j=i,e} I_j = 0, \quad (39)$$

where $I_{i,e}$ are the ion and electron currents to the surface of the dust particles. We note that the widely used theoretical framework for calculation of dust-charging currents is due to the orbit motion limited (OML) theory [50, 51]. We further note that though the general basis for OML theory is not affected by velocity distribution functions obeyed by the electrons ions, the actual expression for currents will get changed by the use of different velocity distribution functions. As such, in our case, while the ion dust-charging current remains same as that for Maxwellian ions, the electron dust-charging current will definitely be different.

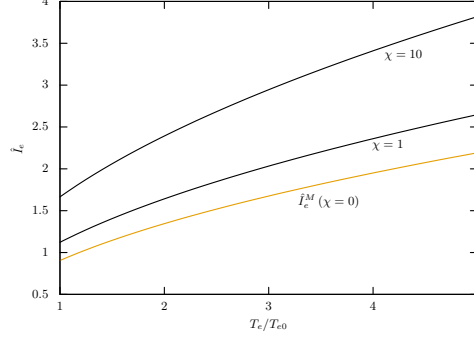


Fig. 2 Electron dust-charging current for electrons with Davydov distribution.

Following the orbit motion limited (OML) theory [50–52], the expressions for I_j for a species ‘ j ’ can be written as (dimensional)

$$I_j = q_j \int_{v_j^{\min}}^{\infty} v_j \Sigma_j f_j(v_j) dv_j, \quad (40)$$

where $f_j(v_j)$ is the velocity distribution function of the corresponding charged particle and

$$\Sigma_j = \pi r_d^2 \left(1 - \frac{2q_j \varphi_d}{m_j v_j^2} \right) \quad (41)$$

is the collision cross-section between a charged particle of charge q_j and a dust particle, where r_d is the radius of a dust-particle and $\varphi_d = \phi_g - \phi$ is the potential of the dust particles with respect to the bulk plasma and ϕ_g being the grain potential. The minimum velocity with which the charged particle approaches a dust particle is given by

$$v_j^{\min} = \left(\frac{2q_j \varphi_d}{m_j} \right)^{1/2}. \quad (42)$$

So, for electrons with Davydov distribution function, we have

$$I_e = -4\pi q r_d^2 n_e \int_{v_e^{\min}}^{\infty} \sigma v^3 f_{e0} dv, \quad (43)$$

where f_{e0} is given by Eq.(15). The above integration can be evaluated analytically and can be written in terms of upper incomplete gamma function $\Gamma(s, x)$

$$I_e = -4\pi r_d^2 e n_e \left(\frac{T_e}{2\pi m_e} \right)^{1/2} \mathcal{F}(e\varphi_d/T), \quad (44)$$

where

$$\mathcal{F}(x) = \frac{(\chi + x)\Gamma(\chi + 1, \chi + x) - \Gamma(\chi + 2, \chi + x)}{e^{-\chi U} \left(-\chi, -\frac{1}{2} - \chi, \chi \right)}. \quad (45)$$

The ion dust-charging current retains its value for Maxwellian distribution function [52]

$$I_i = 4\pi r_d^2 e n_i \left(\frac{T_i}{2\pi m_i} \right)^{1/2} \left(1 - \frac{e\varphi_d}{T_i} \right), \quad (46)$$

In Fig.2, we have shown the plots of I_e as given by Eq.(43) with T_e for different χ and the equivalent expression for Maxwellian electrons I_e^M

$$I_e^M = -4\pi r_d^2 e n_e \left(\frac{T_e}{2\pi m_e} \right)^{1/2} \exp \left(-\frac{e\varphi_d}{T_e} \right). \quad (47)$$

The resultant numerical results indicate that for small φ_d , to a large extent, both the currents differ only by a multiplicative factor and we can express

$$I_e \simeq \beta I_e^M, \quad (48)$$

where β is a constant factor .

Assuming the dust particles to be spherical in size, the net dust-charge $q_d = -ez_d$ can be expressed in terms of dust potential φ_d as

$$q_d = C \Delta V = 4\pi\epsilon_0 r_d \varphi_d, \quad (49)$$

where C is the grain capacitance and. As per our definition

$$z_{d0} = 4\pi\epsilon_0 r_d e^{-1} \varphi_{d0} \quad (50)$$

is the equilibrium dust-charge number at $\phi = 0$, where e is the magnitude of electronic charge. The normalized expression for dust potential is given by

$$\varphi_d = -\alpha^{-1} z_d, \quad (51)$$

where the dust potential is normalized by the magnitude of its equilibrium value φ_{d0} , defined above and α is the magnitude of the inverse of the normalized equilibrium dust potential $\alpha = |\varphi_{d0}|^{-1}$. In normalised form, Eq.(39) can be written as

$$\delta_i \delta_m \sigma^{1/2} n_i \left(1 - \frac{\varphi_d}{\sigma} \right) - \beta n_e e^{\varphi_d} = 0. \quad (52)$$

where $\delta_m = \sqrt{m_e/m_i} \approx 0.023$ and $\sigma = T_{i0}/T_{e0}$ is the ratio of the equilibrium ion temperature to that of the electrons and $\delta_i = n_{i0}/n_{e0}$ is the equilibrium ion to electron density ratio. Using the expression for ion density from Eq.(32), one can solve Eq.(52) for φ_d as a function of ϕ ,

$$\varphi_d(\phi) \simeq \sigma - W \left[\frac{\beta \sigma^{1/2}}{\delta_i \delta_m} e^{\sigma + \phi} \left(1 - \frac{2\phi}{M^2} \right)^{1/2} \right], \quad (53)$$

where $W(z) \equiv W_0(z)$ is the principal branch of Lambert W function. One now needs to solve the integration in Eq.(36) in order to find out the dust contribution to Sagdeev potential, which however *must* be evaluated numerically only. The full charging equation without the involvement of the multiplicative factor β , can however be written in terms of the function $\mathcal{F}(x)$ described above for Davydov electrons as

$$\delta_i \delta_m \sigma^{1/2} n_i \left(1 - \frac{\varphi_d}{\sigma}\right) - n_e \mathcal{F}(-\varphi_d) = 0. \quad (54)$$

This equation however *must* be solved numerically for φ_d . In what follows, we shall approximate the dust potential from Eq.(53), which helps us tackle the problem analytically.

The pseudo-potential has to be evaluated numerically from the following differential equation with the initial condition $V(0) = 0$,

$$\frac{d}{d\phi} V(\phi) = -F(\phi), \quad V(0) = 0, \quad (55)$$

where

$$\begin{aligned} F(\phi) = e^\phi & \frac{U\left(-\chi, -\frac{1}{2} - \chi, -\phi + \chi\right)}{U\left(-\chi, -\frac{1}{2} - \chi, \chi\right)} - \delta_i \left(1 - \frac{2\phi}{M^2}\right)^{-1/2} \\ & - \alpha \delta_d \left(\sigma - W\left[\mathcal{Z} e^\phi \left(1 - \frac{2\phi}{M^2}\right)\right]\right), \end{aligned} \quad (56)$$

where $\alpha = |\varphi_{d0}|^{-1}$ is given by

$$\alpha = |\sigma - W(\mathcal{Z})|^{-1}, \quad (57)$$

$$\mathcal{Z} = e^\sigma \frac{\beta \sigma^{1/2}}{\delta_i \delta_m} \quad (58)$$

6 Solitary waves with dust effects

6.1 The Maxwellian limit ($\chi = 0$) without dust

This is the classical limit for an e - i plasma. In this limit $\chi = 0$ and the function $F(\phi)$ reduces to

$$F(\phi) = e^\phi - \left(1 - \frac{2\phi}{M^2}\right)^{-1/2} \quad (59)$$

and the pseudo-potential can be found analytically as

$$V_{\text{Max}}(\phi) = 1 - e^\phi + M^2 \left(1 - \sqrt{1 - \frac{2\phi}{M^2}}\right). \quad (60)$$

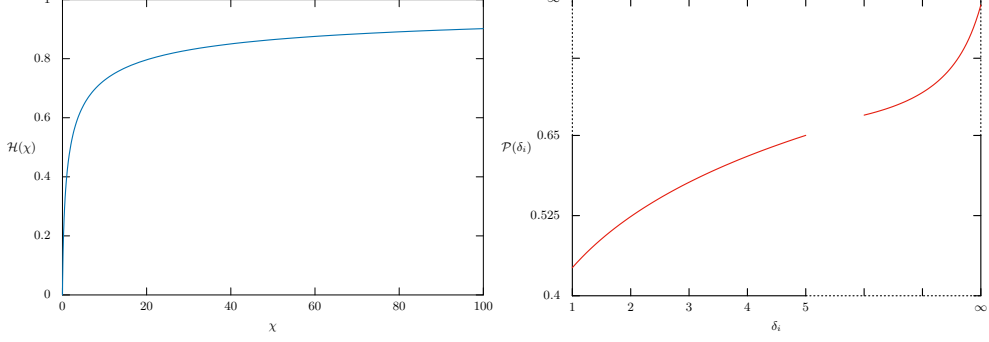


Fig. 3 The functions \mathcal{H} (left) and \mathcal{P} (right for $\beta = 1$).

By expanding the above expression around $\phi = 0$, we can show that $V_{\text{Max}} > 0$ as $\phi \rightarrow \pm 0$ for $M < 1$. For $M > 1$, however V_{Max} always monotonically decreases for $\phi < 0$, so that we can conclude that dark soliton ($\phi < 0$) cannot exist. At the same time, we can also see that for V_{Max} to have a potential structure for $\phi > 0$, M must be > 1 . For ($\phi > 0$), we can readily establish the lower and upper limits for Mach number M

$$1 < M \leq 1.5852. \quad (61)$$

The upper value comes from the fact that for $M \simeq 1.5852$, $V_{\text{Max}}(\phi)$ becomes exactly vertical (slope $\rightarrow \infty$) when simultaneously $V_{\text{Max}}(\phi) = 0$. The value can be found out by equating $\phi \equiv \phi_m = M^2/2$ (the condition for $dV_{\text{Max}}/d\phi \rightarrow \infty$) in Eq.(60) and solve for M . The value of ϕ_m can be found by substituting $M = \sqrt{2\phi_m}$ in Eq.(60), which can be solved analytically

$$\phi_m = -\frac{1}{2} - W_{-1}\left(-\frac{1}{2\sqrt{e}}\right) \simeq 1.2564, \quad (62)$$

with e being the Euler's number and $W_{-1}(z)$ being the negative branch of Lambert W function.

The existence of bright solitons ($\phi > 0$) is shown in Fig.5 in terms of pseudo-potential in Section 6.3, where we have numerically reconstructed the same.

6.2 With Davydov electrons

In order to have an idea of the limits of Mach numbers for Davydov electrons with dust effects, we look at the behavior of the second order derivative of the pseudo-potential at $\phi = 0$, which is given by,

$$V''(0) \equiv \left. \frac{d^2 V}{d\phi^2} \right|_{\phi=0} = -1 + \frac{\delta_i}{M^2} + \mathcal{H}(\chi) - \delta_d \left(1 - \frac{1}{M^2}\right) \mathcal{P}(\delta_i) \quad (63)$$

where

$$\mathcal{H}(\chi) = \chi \frac{U\left(1 - \chi, \frac{1}{2} - \chi, \chi\right)}{U\left(-\chi, -\frac{1}{2} - \chi, \chi\right)}, \quad (64)$$

$$\mathcal{P}(\delta_i) = \frac{W(\mathcal{Z})}{|\sigma - W(\mathcal{Z})|[1 + W(\mathcal{Z})]}. \quad (65)$$

We note that the function $\mathcal{H}(\chi)$ is always bounded in the region $\chi \in [0, +\infty)$ with $0 \leq \mathcal{H}(\chi) < 1$, whereas the function $\mathcal{P}(\delta_i)$ is a positive and monotonically increasing function of δ_i . The balance of these two functions will provide the potential-well nature of the pseudo-potential. The plots of both these functions are shown in Fig.3. Demanding $V'(0) \leq 0$, we get the lower limit for the Mach number

$$M > M_- = \left(\frac{\delta_d \mathcal{P} + \delta_i}{\delta_d \mathcal{P} + 1 - \mathcal{H}} \right)^{1/2}. \quad (66)$$

The upper limit on the Mach number M_+ is given by the expression

$$M_+ = \sqrt{2\phi_{\max}}, \quad (67)$$

where ϕ_{\max} is a solution of the equation $V(\phi) = 0|_{M^2 \rightarrow 2\phi}$. Apparently, this equation in general, can be written as

$$\begin{aligned} & 2\delta_i \phi - \int_0^\phi e^\psi \frac{U\left(-\chi, \frac{1}{2} - \chi, -\psi + \chi\right)}{U\left(-\chi, -\frac{1}{2} - \chi, \chi\right)} d\psi \\ & + \alpha \delta_d \int_0^\phi \left\{ \sigma - W \left[\mathcal{Z} e^\psi \left(1 - \frac{\psi}{\phi} \right)^{1/2} \right] \right\} d\psi = 0. \end{aligned} \quad (68)$$

However, for the existence of M_+ and thereby ϕ_{\max} , the above equation *must* have a real solution $\phi = \phi_{\max} \neq 0$, such that $\chi \geq \phi$ in the domain $\phi \in [0, \phi_{\max}]$.

In the numerical results that we are going to show, we use the constant factor $\beta = 1$, as the important and significant results are always in the region $\delta_i \sim 1$, where $\beta \sim 1$. In Fig.4, we have plotted the M_\pm versus δ_i for various χ . The distinguishing feature for non-Maxwellian electrons ($\chi > 0$) is that both the lower and upper limits of the Mach number decrease with increasing δ_i while for Maxwellian plasma the trend is opposite. We can also see from the plots of M_- , that for $\chi \gtrsim 10$, the Mach number goes beyond 2 and can become more than 3 for higher χ for low dust concentration. As we note that even at high values of $\delta_i \sim 2$, M_- can stay above 2 for higher χ . We can refer to these solitons as *hypersonic* in comparison to a classical Maxwellian *e-i* plasma [48], as the minimum velocity with which these solitons travel is more than

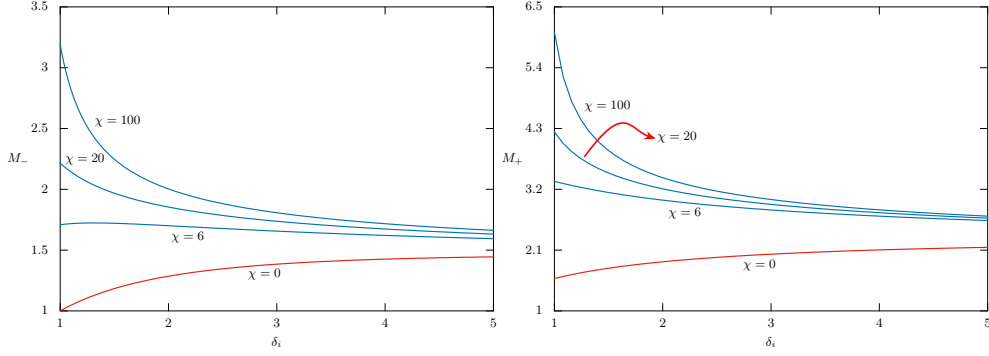


Fig. 4 The lower (M_-) and upper (M_+) limits for the Mach number as dust concentration increases for various values of χ .

twice the ion-sound speed. We also note that for $\delta_i > 1$, such *hypersonic* solitons can also have very large amplitudes. So, there is a possibility of fast-moving large amplitude solitons, reaching large distances, which will eventually dissipate and can give rise to the so-called soliton radiation [20].

In Fig.5, we show the pseudo-potential curves for two cases – Maxwellian electrons ($\chi = 0$) and Davydov electrons with $\chi = 20$. The contrasting behavior of these two cases as already shown in Fig.4, can be seen from the variation of soliton amplitude with δ_i . We note that the soliton amplitude is given by the first zero of the pseudo-potential away from $\phi = 0$. While for Maxwellian electrons the soliton amplitude decreases with increasing dust concentration, it increases for $\chi > 0$. Moreover, as χ increases, the solitons become large but slow down considerably, which can be understood from the conservation of energy. But it is important to note that for lower dust concentration and higher χ , we have $M > 2$. So, high-energy packets of charge-perturbation can travel very fast in this situation.

6.3 Numerical reconstruction of pseudo-potential

As we have seen, for arbitrary (χ, δ_i) , the pseudo-potential has to be constructed numerically. We now outline a procedure, which in general, can be utilized to construct the pseudo-potential with complicated density expressions. This can then be used to solve Poisson's equation. We shall do this through an *inverse mapping* of the electron density function $n_e \equiv F_e(\phi)$ given in Eq.(33). To start with, we consider a mapping of the region in the (χ, ϕ, n_e) space for $\delta_i = 1$. In Fig.6, we show such a mapping, obtained numerically.

It turns out that for any arbitrary χ , the inverse function $F_e^{-1}(n_e)$ can be fitted into an inverse tanh function as

$$\phi \equiv F_e^{-1}(n_e) = \frac{1}{b} \left[\tanh^{-1} \left(\frac{n_e - a_1}{a_2} \right) - a_3 \right], \quad (69)$$

corresponding to map

$$n_e = a_1 + a_2 \tanh(b\phi + a_3), \quad (70)$$

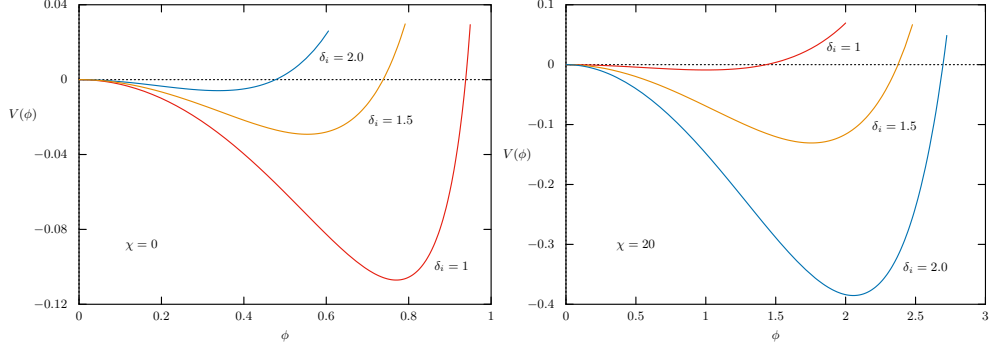


Fig. 5 The pseudo-potential curves for two cases – Maxwellian ($\chi = 0$, left) and Davydov electrons ($\chi = 20$, right) for different δ_i . Note the contrasting behavior of the soliton amplitudes with increasing δ_i in both cases.

where a_i s are constants as determined through the nonlinear fitting. The fitting itself is carried out with the help of the Mathematica algebra system. However, we note that the asymptotic limits of n_e at $\phi \rightarrow (-\infty, 0]$ are $(0, 1]$. Using these values, we see that

$$a_1 = a_2 = a, \quad a_3 = \tanh^{-1} \left(\frac{1}{a} - 1 \right), \quad (71)$$

so that we have the inverse map as

$$\phi = \frac{1}{b} \left[\tanh^{-1} \left(1 - \frac{1}{a} \right) + \tanh^{-1} \left(\frac{n_e}{a} - 1 \right) \right]. \quad (72)$$

This enables us to find out an analytical form for the Sagdeev potential,

$$\begin{aligned} V(\phi) \simeq & M^2 \left[1 - \left(1 - \frac{2\phi}{M^2} \right)^{1/2} \right] - \frac{a}{2b} \log \left(\frac{2a-1}{a^2} \right) - a\phi \\ & - \frac{a}{b} \log \left[\cosh \left\{ b\phi + \tanh^{-1} \left(\frac{1}{a} - 1 \right) \right\} \right]. \end{aligned} \quad (73)$$

At the Maxwellian limit, $a \rightarrow \infty, b \rightarrow 1/2$ and the expression in Eq.(70), $n_e \rightarrow e^\phi$. It can also be seen that for all other cases, we have

$$\infty > a > 1, \quad \frac{1}{2} > b > 0. \quad (74)$$

Computationally, a nonlinear fitting through Eq.(72) for $\chi = 1$, yields $a \simeq 1.44854, b = 0.449851$ for which we have shown the inverse-mapping-computed Sagdeev potential along with the analytically calculated one in Fig.7 (left) which shows an excellent correspondence between the two. The global fitting error remains $\lesssim 10^{-4}$.

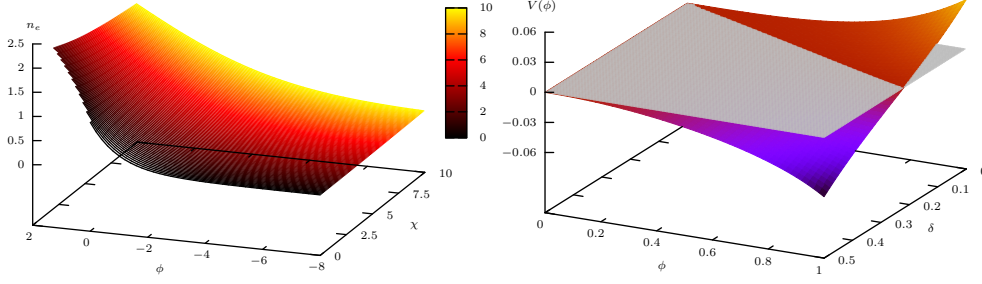


Fig. 6 Electron density n_e as a function of (χ, ϕ) . All the variables are in normalized units (left). The intersection of the $V(\phi) = 0$ plan with surface mapped by (V, δ, ϕ) space for $\delta > 0$ and $\phi > 0$ (right).

To find the limits on M , we carry out a series expansion for $V(\phi)$ as given by Eq.(73) near $\phi \sim 0$, it can be shown that a soliton can exist only if

$$M > M_- = \left(\frac{a/b}{2a-1} \right)^{1/2}, \quad (75)$$

which reduces to the Maxwellian condition $M_-^M = M > 1$ at the limits $a \rightarrow \infty, b \rightarrow 1/2$. This provides us with the lower limit for M . The limit as obtained above is compared to the actual analytical expression given in Eq.(66) in Fig.7 (right).

The derivative of the reconstructed Sagdeev potential with respect to ϕ is given by

$$\frac{d}{d\phi} V(\phi) \equiv V'(\phi) = \left(1 - \frac{2\phi}{M^2} \right)^{-1/2} - a \left[1 + \tanh \left\{ b\phi + \tanh^{-1} \left(\frac{1}{a} - 1 \right) \right\} \right], \quad (76)$$

From the conditions imposed on (a, b) , we can see that for $\phi < 0$,

$$b\phi + \tanh^{-1} \left(\frac{1}{a} - 1 \right) < 0, \quad (77)$$

$$0 \leq 1 + \tanh \left\{ b\phi + \tanh^{-1} \left(\frac{1}{a} - 1 \right) \right\} \leq 1, \quad (78)$$

$$\left(1 - \frac{2\phi}{M^2} \right)^{-1/2} \leq 1, \quad (79)$$

from which, it can be numerically shown that for the intervals $a \in [1, \infty)$ and $b \in (0, 1/2]$

$$V'(\phi) > 0, \quad \forall (a, b), \phi < 0, \quad (80)$$

so that $V(\phi)$ *can not* have any local (or global) maxima for $\phi < 0$ and we conclude that for all values of χ , dark solitons cannot exist.

To see, if we have any upper limit for M , we expand $V(\phi)$ about $M = M_-$

$$V(\phi) \simeq M_-^2(1 - \alpha) - a\phi - \frac{a}{2b} \ln \left[\left(\frac{2a-1}{a^2} \right) \cosh^2 \left\{ b\phi + \tanh^{-1} \left(\frac{1}{a} - 1 \right) \right\} \right]$$

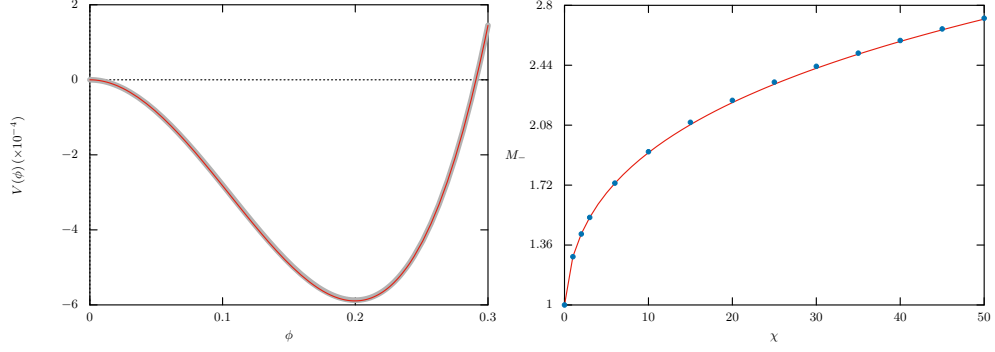


Fig. 7 Left: Reconstructed pseudo-potential through (red solid line) inverse-mapping for $\chi = 1$, superimposed over the analytically calculated one (thick gray line) for $M = 1.4$. Right: The reconstruction of M_- as given by expression (75) shown in circle, superimposed with the analytically calculated M_- from Eq.(66).

$$\begin{aligned}
& + 2M_- \left[1 - \alpha \left(1 + \frac{\phi}{M_-^2 - 2\phi} \right) \right] \delta + \left[1 - \alpha M_-^2 \frac{(M_-^2 - 3\phi)}{(M_-^2 - 2\phi)^2} \right] \delta^2 \\
& - \delta^3 \frac{2\alpha M_- \phi^2}{(M_-^2 - 2\phi)^3} + \mathcal{O}(\delta^4),
\end{aligned} \tag{81}$$

where $\delta = M - M_- > 0$ is the deviation of M from M_- . As $V(\phi) < 0$ in the neighborhood of $\phi \sim 0$ for $M > M_-$, it must be again positive for a certain value of $\phi = \phi_m$ away from $\phi = 0$ for a soliton to exist. It can now be numerically shown that the surface mapped by (V, δ, ϕ) space for $\delta > 0$ and $\phi > 0$ intersects with the $V(\phi) = 0$ plan only when $\delta \rightarrow \delta_{\max}$, as shown in Fig.6 (right) This shows that there exists an upper value for $M = M_+ \simeq M_- + \delta_{\max}$ for the existence of solitons.

7 Conclusion

To summarize, we have considered the possibility of the formation of electrostatic solitons in a plasma environment, which is characterized by MRI-driven turbulent heating of the electrons, making the electrons obey a non-Maxwellian velocity distribution, particularly the so-called Davydov distribution. The electron distribution becomes Maxwellian when the heating is neglected and becomes a Druyvesteyn distribution function [42] in the extreme case. The plasma itself is described by such electrons, a Maxwellian ion fluid and negatively charged dust grains. The dust grains are assumed to be static in the ion-acoustic timescale and ion temperature is neglected in comparison to that of the electrons. We show that the situation for such a condition is favorable in the plasma environment of a PPD, specifically in the MRI-stable dead zones, which are rife with turbulence-driven random heating. We show that electrostatic nonlinear structures, in these situations, can form with very large velocities, often crossing several orders of magnitude larger than the ion-sound speed. These fast-moving solitons can also be of quite high amplitudes. We argue that these solitons can be an effective mechanism for energy equilibration through a

process known as soliton radiation. One of the interesting findings of this analysis is that the behavior of soliton velocity (the Mach number) with dust density reverses as the electron velocity distribution deviates more from Maxwellian. We have however neglected the dust-charge fluctuation and assumed that the net current to the dust particles is always zero. It is to be also noted that χ , which is a measure of how high is the heating, can be easily estimated to reach up to about ~ 100 [13], making the electron highly non-Maxwellian. With relevant parameters for PPDs, we find the soliton velocity in extreme cases can become more than $\sim 4 - 5$ times the ion-sound speed and their amplitudes can reach up to several hundreds of Debye length.

We have also outlined a procedure to facilitate analytical analysis of the resultant pseudo-potential through an inverse-mapping of the electron density with plasma potential. This procedure makes the analysis easier where an analytic treatment of the densities in terms of plasma potential is not otherwise feasible due to their complicated expressions, such as one encountered in this work.

Acknowledgement

It is a pleasure to thank the anonymous referees for their suggestions, which have greatly improved the manuscript.

Declarations

Author Contributions: All authors contributed equally.

Data Availability Statement: No Data associated in the manuscript.

Conflicts of Interest: The authors declare no conflict of interest.

References

- [1] Pringle, J.E. Ann. Rev. Astron. Astrophys. **19**, 137 (1981)
- [2] Mamajek, E.E., Meyer, M.R., Hinz, P.M., Hoffmann, W.F., Cohen, M., Hora, J.L. Astrophys. J. **612**, 496 (2004)
- [3] White, R.J., Hillenbrand, L.A. Astrophys. J. **621**, 65 (2005)
- [4] Armitage, P.J. Ann. Rev. Astron. Astrophys. **49**, 195 (2011)
- [5] Lesur, G.R.J. J. Plasma Phys. **87**, 205870101 (2021)
- [6] Muranushi, T. Mon. Not. R. Astron. Soc. **401**, 2641 (2010)
- [7] Akimkin, V., Ivlev, A.V., Caselli, P., Gong, M., Silbee, K. Astrophys. J. **953**, 72 (2023)
- [8] Balbus, S.A., Hawley, J.F. ApJ **376**(214) (1991)

- [9] Hawley, J.F., Gammie, C.F., Balbus, S.A. *ApJ* **440**(742) (1995)
- [10] Gammie, F.C. *Astrophys. J.* **457**, 355 (1996)
- [11] Wardle, M. *Astrophys. J. Suppl.* **311**, 35 (2007)
- [12] Inutsuka, S.-I., Sano, T. *ApJL* **628**(L155) (2005)
- [13] Okuzumi, S., Inutsuka, S.-I.I. *Astrophys. J.* **800**(47) (2015)
- [14] Golant, V.E., Zhilinsky, A.P., Sakharov, I.E.: *Fundamentals of Plasma Physics*. Wiley, New York (1980)
- [15] Lifshitz, E.M., Pitaevskii, L.P.: *Physical Kinetics* vol. 10. Pergamon Press, Oxford (1981)
- [16] Davydov, B. *Phys. Z. Sowjet.* **8**(59) (1935)
- [17] Galeev, A.A., Sagdeev, R.Z. *Rev. Plasma Phys.* **7**, 1 (1979)
- [18] Kuznetsov, E.A., Rubenchik, A.M., Zakharov, V.E. *Phys. Rep.* **142**(3), 103 (1986)
- [19] Karpman, V.I., Schamel, H. *Phys. Plasmas* **4**, 120 (1997)
- [20] Murusidze, I.G., Tsintsadze, N.L., Tskhakaya, D.D., Shukla, P.K. *Phys. Scr.* **58**, 266 (1998)
- [21] Antonova, E.E. *Adv. Space Res.* **41**(10), 1677 (2008)
- [22] Rubinstein, R., Clark, T.T. *Theor. Appl. Mech. Lett.* **7**, 301 (2017)
- [23] Böhm-Vitense, E.: *Introduction to Stellar Astrophysics. Stellar atmospheres*, vol. 2. CUP, Cambridge (1997)
- [24] Levich, E. *Ann. N. Y. Acad. Sci.* **404**(1), 73 (1983)
- [25] Levich, E. *Concepts Phys.* **6**(3), 239 (2009)
- [26] Lee, C.B. *Phys. Rev. E* **62**, 3659 (2000)
- [27] C. b. lee and j. z. wu. *Appl. Mech. Rev.* **61**, 030802 (2008)
- [28] Lee, C.B., Jiang, X.Y. *Phys. Fluids* **31**, 111301 (2019)
- [29] Jiang, X.Y., Lee, C.B., Chen, X., Smith, C.R., Linden, P.F. *J. Fluid Mech.* **890**, 11 (2020)
- [30] Hopfinger, E.J., Browand, F.L. *Nature* **295**, 393 (1982)

- [31] Mozer, F.S., Bonnell, J.W., Hanson, E.L.M., Gasque, L.C., Vasko, I.Y. *Astrophys. J.* **911**, 89 (2021)
- [32] Temerin, M., K, C., Lotko, W., Mozer, F.S. *Phys. Rev. Lett.* **48**, 1175 (1982)
- [33] al., S.J.Z. *Nucl. Fusion* **44**, 134 (2004)
- [34] Zweben, S.J., Liewer, P.C., Gould, R.W. *Bull. Am. Phys. Soc.* **27**, 973 (1982)
- [35] Surko, C.M., Slusher, R.E. *Bull. Am. Phys. Soc.* **27**, 937 (1982)
- [36] Meiss, J.D.: *Statistical Physics and Chaos in Fusion Plasmas. Nonequilibrium Problems in the Physical Sciences and Biology*, vol. 3. Wiley–Blackwell, New Jersey (1984)
- [37] Wang, R., Vasko, I.Y., Mozer, F.S., Bale, S.D., Artemyev, A.V., Bonnell, J.W., Ergun, R., Giles, B., Lindqvist, P.-A., Russell, C.T., Strangeway, R. *Astrophys. J. Lett.* **889:L9** (2020)
- [38] Burch, J.L., Moore, T.E., Torbert, R.B., Giles, B.L. *Space Sci. Rev.* **199**, 5 (2016)
- [39] Das, M., Bora, M.P. arXiv:2402.18478 [physics.plasm-ph] (2024)
- [40] Korteweg, D.J., Vries, G. *Phil. Mag.* **39**, 422 (1895)
- [41] Peregrine, D.H. *J. Fluid Mech.* **25**(2), 321 (1966)
- [42] Druyvesteyn, M.J., Penning, F.M. *Rev. Mod. Phys.* **12**(87) (1940)
- [43] Khusroo, M.: A study on plasma processes in astrophysical environment with an emphasis on magnetospheres and accretion disks. PhD thesis, Gauhati University, <http://hdl.handle.net/10603/291394> (2019)
- [44] Frost, L.S., Phelps, A.V. *Phys. Rev.* **127**, 1621 (1962)
- [45] Yoon, J.-S., Song, M.-Y., Han, J.-M., Hwang, S.H., Chang, W.-S., Lee, B., Itikawa, Y. *J. Phys. Chem. Ref.* **37**, 913 (2008)
- [46] Gubbins, D., Herrero-Bervera, E. (eds.): *Encyclopedia of Geomagnetism and Paleomagnetism*, 1st edn. Springer, Dordrecht (2007)
- [47] Sano, T., Stone, J.M. *Astrophys. J.* **577**, 534 (2002)
- [48] Chen, F.F.: *Introduction to Plasma Physics and Controlled Fusion* vol. 1, 2nd edn. Plenum Press, New York and London, New York (1974)
- [49] Sagdeev, R.Z. *Rev. Mod. Phys.* **51**, 1 (1979)
- [50] Mott-Smith, H., Langmuir, I. *Phys. Rev.* **28**, 0727 (1926)

- [51] Allen, J.E. Phys. Scripta **45**, 497 (1992)
- [52] Shukla, P.K., Mamun, A.A.: Introduction to Dusty Plasma Physics. IOP, Bristol and Philadelphia (2002)